

Evaluation of Performance of the MACAO Systems at the VLTI

Sridharan Rengaswamy^a, Pierre Haguenaer^a, Stephane Brillant^a, Angela Cortes^a, Julien H. Girard^a, Stephane Guisard^b, Jérôme Paufique^b, Andres Pino^a

^aEuropean Southern Observatory (ESO), Casilla 19001, Vitacura, Santiago, Chile

^bEuropean Southern Observatory (ESO), Karl-Schwarzschildstr. 2, D-85748, Garching, Germany

ABSTRACT

Multiple Application Curvature Adaptive Optics (MACAO) systems are used at the coude focus of the unit telescopes (UTs) at the La-Silla Paranal Observatory, Paranal, to correct for the wave-front aberrations induced by the atmosphere. These systems are in operation since 2005 and are designed to provide beams with 10 mas residual rms tip-tilt error to the VLTI laboratory. We have initiated several technical studies such as measuring the Strehl ratio of the images recorded at the guiding camera of the VLTI, establishing the optimum setup of the MACAO to get collimated and focused beam down to the VLTI laboratory and to the instruments, and ascertaining the data generated by the real time computer, all aimed at characterizing and improving the overall performance of these systems. In this paper we report the current status of these studies.

Keywords: Adaptive Optics, Curvature sensor, MACAO

1. INTRODUCTION

Four Multiple Application Curvature Adaptive Optics systems have been developed and deployed at the ESO's Very Large Telescope Interferometer.^{1,2} These systems, conveniently placed at the coude focus on movable translation stages (X-Y tables), were designed to provide a K-band Strehl of $> 50\%$ for $V < 8$, $>25\%$ for $V = 15.5$ (at a seeing of $0.65''$ with a wind speed of 10 m/s) and a residual rms wave-front tip/tilt of less than 10 mas for the beams entering the VLTI laboratory. These systems use a 60 element bimorph deformable mirror for wavefront correction and a loudspeaker driven membrane mirror for wavefront sensing. The telescope beam is focused on membrane mirror with a telecentric lens and then collimated onto a 60 element lenslet array, through a prismatic derotator to compensate the rotation between the deformable mirror and the lenslet array, and then imaged onto 60 avalanche-photo-diodes (APDs) through a fiber-optic bundle. The membrane mirror vibrates at 2.1 kHz rate, but the curvature signals are integrated over 5 cycles and thus effectively the wavefront curvature sensing and correction are done at 420 Hz. These systems are used for coude guiding when the VLTI is used with the UTs, for about a week every month. In view of the regular use of these systems, it is necessary to perform periodical tests to evaluate and monitor their performances. In this paper, we report two such activities carried out during the last year.

2. STREHL RATIO OF THE IMAGES ON IRIS

IRIS is an infra-red image stabilization system located in the VLTI laboratory . It corrects for the movement of the image barycenter (arising from the turbulence in the VLTI tunnel and residual aberrations after MACAO correction) of the beams entering the VLTI laboratory. The stellar beams are imaged on one of the four quadrants of the IRIS camera. For each instrument, a reference pixel that maximizes the flux at its detector plane, is defined for each quadrant, representing the optical axis of the VLTI. The photo-centers of the images are measured for every detector integration time (DIT) and are used to control the fast tip-tilt actuators of the instruments and for slow offload to the telescope axes. Measuring the Strehl ratio of the images at the IRIS quadrants will provide effective Strehl ratio that can be expected at the instrument focal plane as it includes the effect of the tunnel seeing as well.

Further author information: (Send correspondence to R. Sridharan)

R. Sridharan: E-mail: srengasw@eso.org, Telephone: +56 2 463 3084

2.1 Data

We observed several stars, with R magnitude from 12 to 17.6. After closing the AO loop, we recorded a series of IRIS images for about a minute (about 420 frames) in PSF/TTS mode, for each star. We also recorded a series of background images, and some auxiliary data containing coherence time, airmass etc., immediately after observing the star. For each star, observations were performed near simultaneously on MACAO1 and MACAO2, on July 7, 2009, and on MACAO2 and MACAO3 on September 4, 2009. On July 8, stand-alone observations were performed with MACAO4.

2.2 Analysis

We used the Strehl Ratio (SR) as a metric to characterize the closed loop performance of the system. Measuring the SR on near simultaneously recorded images of two MACAOs helps us to evaluate their relative performances. The following procedure was used to estimate the Strehl ratio from the recorded IRIS images (which were of the size of 128×128 pixels; 1 pixel = 36 mas in TTS mode, 8.23 mas in PSF mode) in K band.

1. A mean background image was estimated from the series of about 100 background images after removing hot-pixels from the individual frames.
2. Hot pixels were removed from each of the target images (about 420 frames in total) and then the mean background image was subtracted from each of them.
3. In each background subtracted image, pixels having negative intensity were replaced with zeros. The residual isolated hot pixels, if any, were replaced by the mean intensity of the pixels surrounding them.
4. Each image was with an exposure time of 66 ms. 15 such “corrected” images were averaged to obtain a “long exposure” image. Strehl Ratio was estimated for this long exposure image. As the data contained about 420 images, we obtained a series of about 28 SRs for each star and estimated a mean and standard deviation from them. Individual SRs were estimated using two equivalent methods: (a) The peak intensity of the average image was divided by the peak intensity of a synthetic point spread function generated with an outer diameter of 811.5 cm and an inner diameter of 111.6 cm. (b) Each average image (PSF, area normalized) was Fourier transformed to get the optical transfer function (OTF), and then the volume under the OTF was divided by the theoretical volume under OTF estimated from the synthetic PSF to obtain the SR.

2.3 Results

As mentioned earlier, the MACAO systems were designed for a seeing of better than $0.65''$. However during our observations, the seeing was mostly worse than $1''$. Thus, it was hard to compare the SRs with the original design specifications. Thus, we only present the relative performance of the MACAO systems here. One of our aims was to focus on the performance of MACAO2 which, in the past, had shown poorer performance than the other MACAO systems. We characterized the relative performance of MACAO2, by normalizing the SRs obtained from MACAO2 by those of MACAO1 and MACAO3 (which were set to unity for the sake of convenience). Our other objective was to establish the limiting magnitude of all the MACAOs. This was triggered by the fact that MACAO4 failed to close the loop on targets of magnitude around 16 during normal operations.

2.3.1 Relative performance of the MACAOs

Figure 1 shows a plot of the relative SR as a function of the stellar magnitude, for MACAOs 1 and 2. The green diamond symbol indicates SR for MACAO1 (forcefully set to unity) and the red diamond symbol indicates the relative SR for MACAO2. The atmospheric seeing remained more or less constant (about $1''$) during the observations. We find that under the given seeing conditions, the performance of MACAO2 is not drastically different from MACAO1 indicated by the fact that the relative SR is better than 0.5 always. At the same time, it should also be noticed that the performance of MACAO2 is always slightly worse than that of MACAO1. As of now, with the present data, it is not clear whether the observed differences in SRs are significant or not, given the fact that the MACAO systems are not really optimized for seeing conditions worse than $0.65''$. In

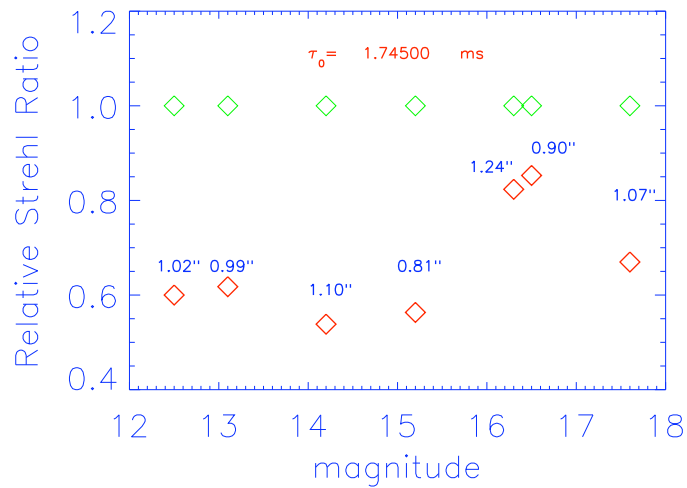


Figure 1. Comparison of SR estimated from near-simultaneous IRIS images corrected by MACAO1 and MACAO2. The SRs obtained with MACAO2 have been normalized by dividing them by the SRs obtained with MACAO1. The green diamond symbol indicates SR for MACAO1 (forcefully set to unity) and the red diamond symbol indicates the normalized SR for MACAO2. The seeing (an average of the instances at which MACAO1/MACAO2 data were recorded) is also indicated; it remained constant at about 1 arcsec throughout the observations. The coherence time was between 1 to 2 ms. The performance of MACAO2 is always slightly inferior to that of MACAO1.

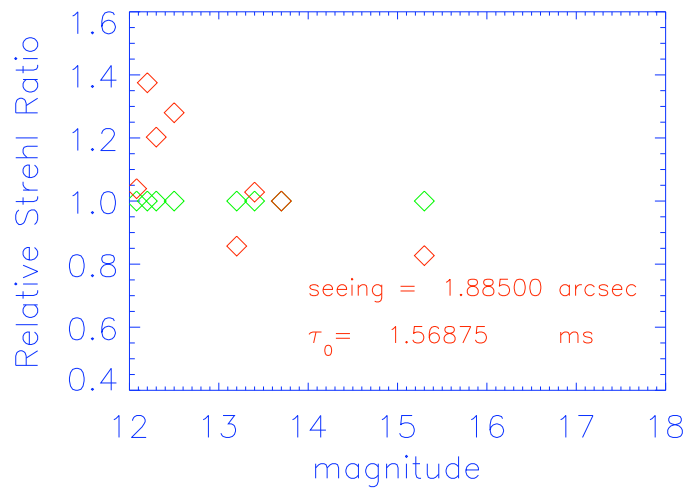


Figure 2. Comparison of SR estimated from near-simultaneous IRIS images corrected by MACAO2 and MACAO3. The SRs obtained with MACAO2 have been normalized by dividing them by the SRs obtained with MACAO3. The green diamond symbol indicates SR for MACAO3 (forcefully set to unity) and the red diamond symbol indicates the normalized SR for MACAO2. The seeing varied from 1.6" to 2.2" with an average value of 1.88". The coherence time was between 1.4 to 1.7 ms with the mean of 1.56 ms

other words, we will have to see how the systems compare under good seeing conditions of 0.4"-0.5". It was also observed that a slight change of loop gain values causes small differences in the SR.

Figure 2 shows the SR obtained with MACAO2 and MACAO3. It clearly indicates that the performance of

MACAO2 and MACAO3 are similar under identical conditions.

2.3.2 Limiting magnitude of the MACAOs

During the technical tests carried out in July and September 2009, we found that MACAO loop could be closed even on stars as faint as $R = 17.6$ consistently (twice on MACAO2 and MACAO1, once in MACAO4), at seeing of about $1''$. This indicates that the earlier observation of MACAO loop not closing at $V=16$ must be an isolated event (perhaps due to momentarily bad seeing and/or very low coherence time). Moreover, it would be essential to know the R magnitude rather than the V magnitude. In order to investigate further, we now record MACAO data regularly during VLTI.UT runs, and this will enable us to establish the limiting magnitude on a statistical basis.

2.3.3 SR vs coherence time

Figure 3 shows a plot of the SR vs coherence time from the measurements made on all the MACAOs. The MACAO systems were designed for a seeing of better than $0.65''$. As most of the observations presented here correspond to seeing of worse than $1''$, these can not be representative of the real performance under good seeing conditions.

The results presented here (SR) were obtained without correcting IRIS images for image motion. It is found that a slightly higher SR can be obtained if the IRIS images were corrected (through software) for tip/tilt motion. The increase in SR is itself proportional to the target's brightness. For bright stars ($R=2.5$) there is almost no difference between tip/tilt corrected and uncorrected IRIS images. However, for faint targets ($R > 14$) SR increases by about 0.02, on an average.

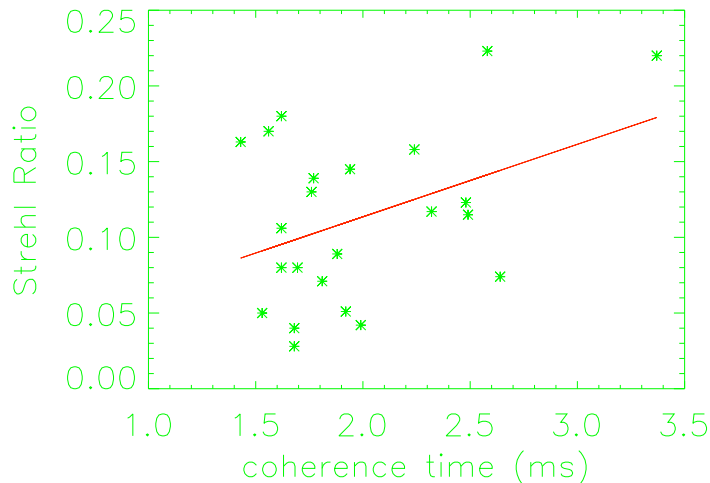


Figure 3. A plot of SR as a function of coherence time. Although there is an indication that higher SRs can be obtained with higher coherence times, the relation is not strictly linear. The SRs are rather low and mostly correspond to seeing of worse than $1''$, while the MACAOs were originally designed for a seeing of better than $0.65''$.

3. MEASUREMENT OF MACAO MEMBRANE POSITION OFFSETS

Ever since the MACAOs were installed, the position of the membrane mirrors have been adjusted by a few millimeters to obtain the best focused images on the IRIS inside the VLTI laboratory. Recently, these position offsets were re-established with a better accuracy. The focus of the IRIS has been adjusted using the focus reference of the VLTI installed on the VLTI beam compressors table and hence can be considered as a good reference of focus.

3.1 Measurement procedure

The measurements were done during daytime using the Nasmyth beacon as a source. The light of each telescope was sent to the VLTI following the normal VLTI path and with the same association of the delay lines to the UTs as done during the normal (night) operation. The UT beams were also associated with similar input channels as done during the normal operations. The delay lines were positioned and the variable curvature mirrors were inflated accordingly to re-image the pupil inside the VLTI laboratory. The beacon brightness level was adjusted to have a correct flux level on the IRIS. With the AO loop closed, the XY table position was adjusted to center the beacon image on the IRIS reference pixel (64,64). The M10 angular position was adjusted to center the pupil on the reference pixels of the ARAL (ARtificial source ALignment unit). The M10 longitudinal position was set to the nominal position defined by the coude optical train alignment, for all the MACAOs. Two different methods were adopted to establish the correct offset position of the membrane mirror.

Method 1: The membrane position was offseted from 0 to 30 mm (maximum range) in steps of 2.5 mm. At each offset position, a series of IRIS images were recorded after centering the image on the reference pixel. The measurement procedure was repeated for two different positions of the delay line, namely at 14 m and at 100 m.

Method 2: In this method, in addition to varying the position of the membrane mirror from 0 to 30 mm in steps of 2.5 mm, a 2 Hz sinusoidal modulation of focus was added to the deformable mirror, with the maximal amplitude allowed by the MACAO tool. Again, a series of images were recorded after centering the images on the reference pixel. This method was applied only to the MACAO2.

3.2 Results

The SR was measured from each recorded image on all of the IRIS quadrants (which correspond to different MACAOs), for each membrane position. The individual images were inspected for saturation and thus the possibility of biasing the SR was avoided. For the first method, the average and standard deviation of the SRs were estimated for two positions of the delay lines. Figures 4 to 7 indicate the results for each individual UTs. The series of points (SRs) were fitted with a polynomial curve to determine the position of the membrane giving the best focus. The results are indicated in Table 1.

	Membrane position with DL 14m (mm)	Membrane position with DL at 100m	Mean position (mm)	Membrane position for M10 (mm)
UT1	4.4	4.8	4.6	12.89
UT2	26.4	26.8	26.6	17.96
UT3	25.2	25.7	25.5	24.58
UT4	6.8	6.7	6.8	8.47

Table 1. MACAO membrane offset positions for best focus on the IRIS.

For the second method, the best focus position was obtained through a Fourier analysis of the SRs. When the membrane is away from the position that would provide good focus on the IRIS, the Fourier transform of the SRs shows a peak at the frequency of the focus modulation of the deformable mirror. As the membrane offset approaches close to the position that provides the best focus on the IRIS, the peak at the 2Hz decreases and a peak at 4 Hz starts appearing. When the position of the membrane mirror provides the best focused images on the IRIS, the peak at 2Hz disappears completely and only the peak at 4Hz remains. Thus, the ratio of the peaks at 4 Hz and 2 Hz is a measure of best focus position. As shown in top left panel of Figure 8, the ratio of the peaks suddenly increases at the best membrane offset position. As an illustration of the method, computed series of Strehl Ratios are plotted for membrane positions of 15 mm (lower right), 27.5 mm (lower left) and 25 mm (upper right). We see only the modulation frequency when the membrane offset is 15 mm (bad focus). As the membrane offset approaches the best position (27.5 mm), double frequency starts appearing, and at the offset position (25 mm) only the double frequency appears. The robustness of the second method is that the ratio of the power spectrum peaks sharply increases at the position that provides the best focus on the IRIS and thus, leads to a clear identification.

The results mentioned above would lead to the conclusion that the VLTI beams are correctly collimated between M10 and IRIS. This shall be confirmed by verification with the optical design, of how a defocus in the

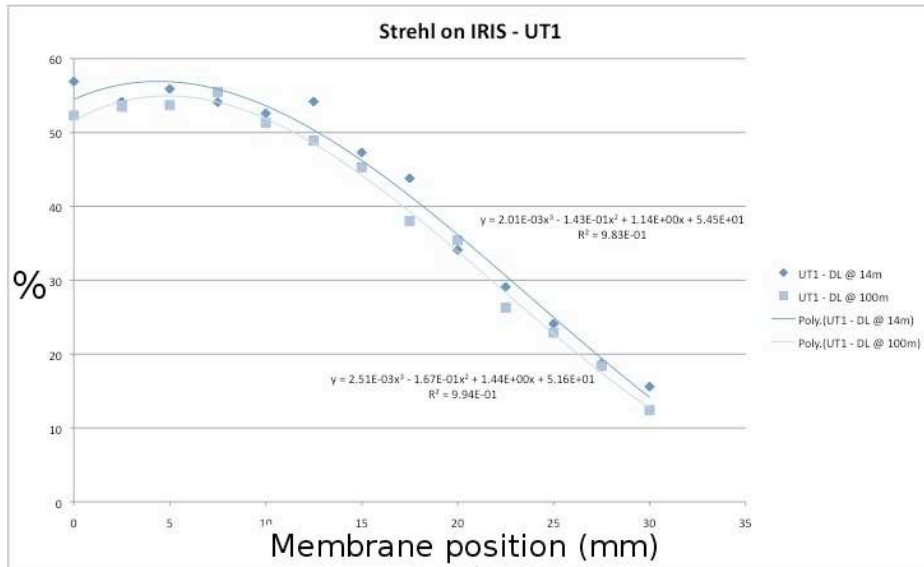


Figure 4. Strehl Ratio measured on the IRIS images for UT1, vs. the membrane position, for DL position of 14 m and 100 m.

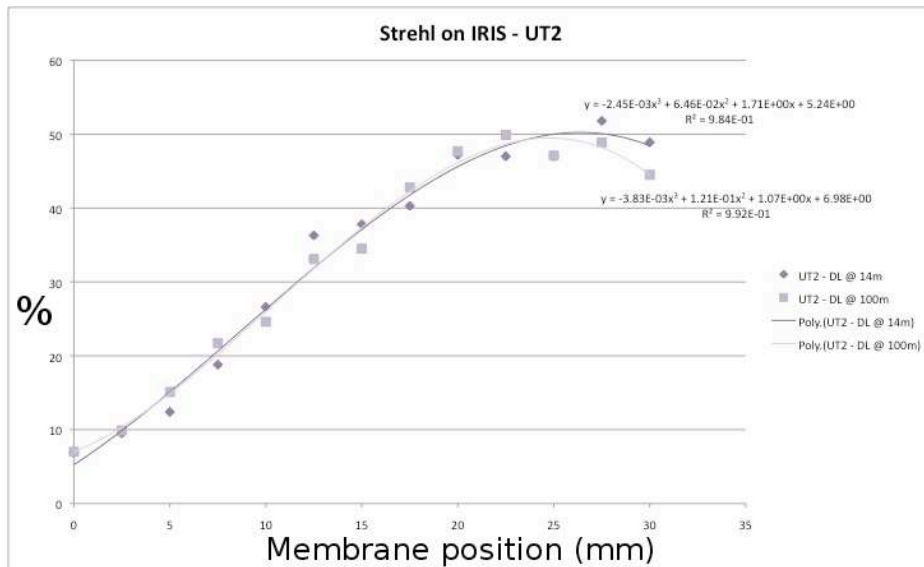


Figure 5. Strehl Ratio measured on the IRIS images for UT2, vs. the membrane position, for DL position of 14 m and 100 m.

VLT train after M10 would add to a defocus before M10. The measured membrane offset positions are in good agreement with the ones measured for the M10 in June 2007 for UT3 and UT4. For UT1 and UT2, they differ significantly, and this is still under investigation.

4. SUMMARY

We have presented the relative Strehl Ratios obtained on the IRIS images for MACAO1, MACAO2 and MACAO3. The performance of MACAO2 is slightly inferior to that of MACAO3 and there is no significant difference in terms of the SR. The poor performance of MACAO2 in the past is perhaps due to the fiber misalignment, which has been rectified now. The limiting magnitudes of MACAO4 (and hence of all the MACAOs) is about

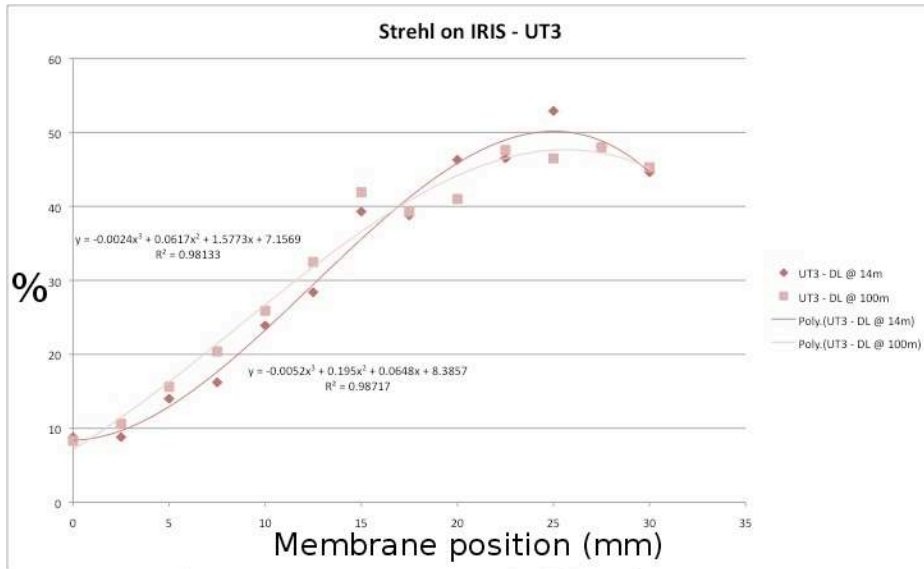


Figure 6. Strehl Ratio measured on the IRIS images for UT3, vs. the membrane position, for DL position of 14 m and 100 m.

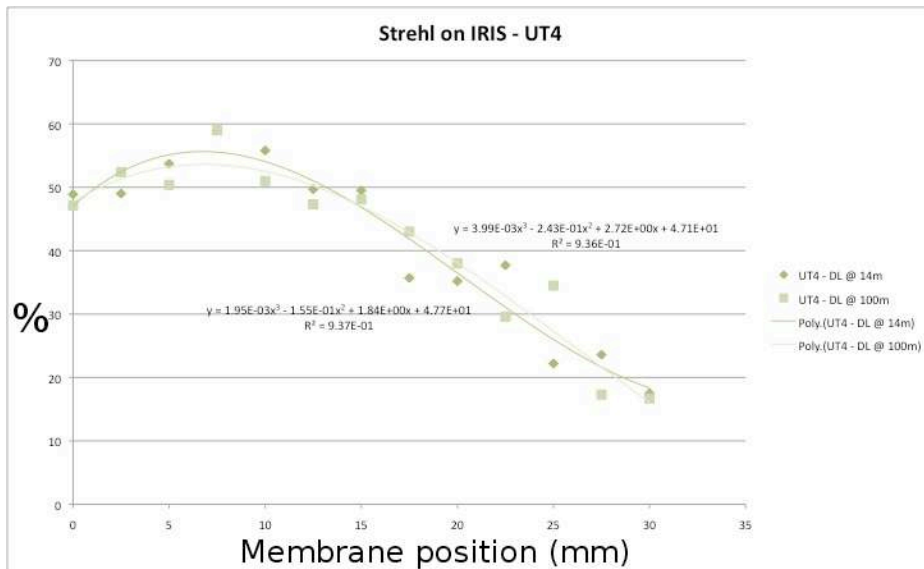


Figure 7. Strehl Ratio measured on the IRIS images for UT4, vs. the membrane position, for DL position of 14 m and 100 m.

17, although a few isolated cases of adaptive optics loop opening at brighter targets have been reported. The MACAO membrane offset positions have been re-established to achieve the best focus on the IRIS inside the VLTI laboratory. In the near future, we plan to re-establish and optimize the control loop gain (integral), and re-measure the influence functions of the deformable mirrors. The data used for this study were limited and hence do not provide the complete characterization of the systems. We have already started recording the MACAO real time computer data during normal operations in all the MACAOs and this will enable us to evaluate and monitor the performances on a statistical basis under different seeing conditions.

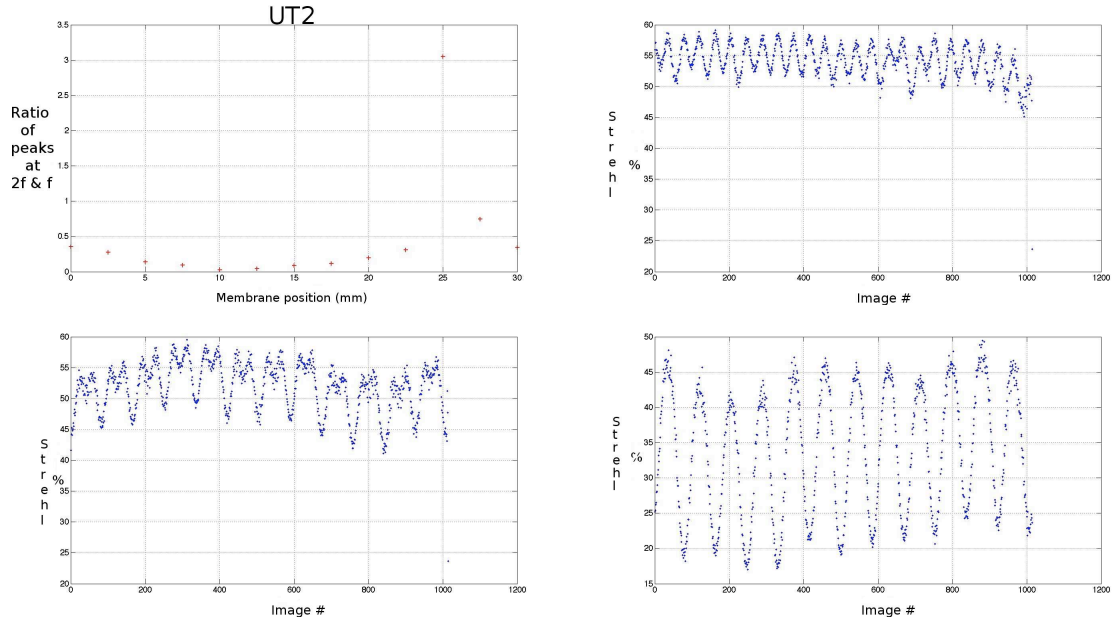


Figure 8. Focus modulation induced on the MACAO2 deformable mirror to obtain the best membrane offset position that produces the best focus on the IRIS. Top left: The ratio of the peaks at 4Hz and 2Hz rapidly increases as the correct membrane position is approached. Top right: Only double the frequency is seen at 25 mm. Bottom left: Both the double frequency, actual frequency appear. Bottom right: Only modulation frequency appears when the membrane position is far from the correct position (that gives best focus on IRIS).

ACKNOWLEDGMENTS

We thank the director of the La-Silla Paranal Observatory for granting us technical time to perform the studies reported in this paper.

REFERENCES

- [1] Arsenault, R., Donaldson, R., Dupuy, C., Fedrigo, E., Hubin, N., Ivanescu, L., Kasper, M., Oberti, S., Paufigue, J., Rossi, S., Silber, A., B. Delabre, Lizon, J. L., and Gigan, P., “Macao-vlti adaptive optics systems performance,” in *[Advancements in Adaptive Optics]*, Calia, D. B. and Ellerbroek, B. L., eds., *Proc. SPIE* **5490**, 47–58 (2004).
- [2] Arsenault, R., Alonso, J., Bonnet, H., Brynnel, J., Delabre, B., Donaldson, R., Dupuy, C., Fedrigo, E., Farinato, J., Hubin, N., Ivanescu, L., Kasper, M., Paufigue, J., Rossi, S., Tordo, S., Stroebele, S., Lizon, J. L., Gigan, P., Delplanche, F., Silber, A., Quattri, M., and Reisse, R., “Macao-vlti: An adaptive optics system for the eso interferometer,” in *[Adaptive Optical System Technologies II]*, P. L. Wizinowich, D. B., ed., *Proc. SPIE* **4839**, 174–185 (2003).